

## Long Pulse operation with the ITERRelevant LHCD Antenna in Tore Supra

A. Ekedahl, L. Delpech, M. Goniche, D. Guilhem, J. Hillairet et al.

Citation: [AIP Conf. Proc. 1406](#), 399 (2011); doi: 10.1063/1.3665002

View online: <http://dx.doi.org/10.1063/1.3665002>

View Table of Contents: <http://proceedings.aip.org/dbt/dbt.jsp?KEY=APCPCS&Volume=1406&Issue=1>

Published by the American Institute of Physics.

---

### Related Articles

Full-wave modeling of the O–X mode conversion in the Pegasus toroidal experiment  
[Phys. Plasmas 18](#), 082501 (2011)

Validation of on- and off-axis neutral beam current drive against experiment in DIII-D  
[Phys. Plasmas 16](#), 092508 (2009)

Temperature and density characteristics of the Helicity Injected Torus-II spherical tokamak indicating closed flux sustainment using coaxial helicity injection  
[Phys. Plasmas 15](#), 082501 (2008)

Field-reversed configuration formation scheme utilizing a spheromak and solenoid induction  
[Phys. Plasmas 15](#), 032503 (2008)

Rotating magnetic field current drive of high-temperature field reversed configurations with high  $\zeta$  scaling  
[Phys. Plasmas 14](#), 112502 (2007)

---

### Additional information on AIP Conf. Proc.

Journal Homepage: <http://proceedings.aip.org/>

Journal Information: [http://proceedings.aip.org/about/about\\_the\\_proceedings](http://proceedings.aip.org/about/about_the_proceedings)

Top downloads: [http://proceedings.aip.org/dbt/most\\_downloaded.jsp?KEY=APCPCS](http://proceedings.aip.org/dbt/most_downloaded.jsp?KEY=APCPCS)

Information for Authors: [http://proceedings.aip.org/authors/information\\_for\\_authors](http://proceedings.aip.org/authors/information_for_authors)

---

### ADVERTISEMENT

The advertisement features the AIP Advances logo on the left, consisting of the word "AIP" in blue and "Advances" in green, with several orange spheres of varying sizes floating above it. Below the logo is a green button with the text "Submit Now". To the right, there is a large green area containing promotional text and bullet points.

**Explore AIP's new open-access journal**

- Article-level metrics now available
- Join the conversation! Rate & comment on articles

# Long Pulse operation with the ITER-Relevant LHCD Antenna in Tore Supra

A. Ekedahl<sup>1</sup>, L. Delpech<sup>1</sup>, M. Goniche<sup>1</sup>, D. Guilhem<sup>1</sup>, J. Hillairet<sup>1</sup>,  
M. Preynas<sup>1</sup>, P.K. Sharma<sup>2</sup>, J. Achard<sup>1</sup>, Y.S. Bae<sup>3</sup>, X. Bai<sup>4</sup>, C. Balorin<sup>1</sup>,  
Y. Baranov<sup>5</sup>, V. Basiuk<sup>1</sup>, A. Bécoulet<sup>1</sup>, J. Belo<sup>6</sup>, G. Berger-By<sup>1</sup>,  
S. Brémond<sup>1</sup>, C. Castaldo<sup>7</sup>, S. Ceccuzzi<sup>7</sup>, R. Cesario<sup>7</sup>, E. Corbel<sup>1</sup>,  
X. Courtois<sup>1</sup>, J. Decker<sup>1</sup>, E. Delmas<sup>8</sup>, B.J. Ding<sup>9</sup>, X. Ding<sup>4</sup>, D. Douai<sup>1</sup>,  
R. Dumont<sup>1</sup>, C. Goletto<sup>1</sup>, J.P. Gunn<sup>1</sup>, P. Hertout<sup>1</sup>, G.T. Hoang<sup>1</sup>,  
F. Imbeaux<sup>1</sup>, K. Kirov<sup>5</sup>, X. Litaudon<sup>1</sup>, P. Lotte<sup>1</sup>, P. Maget<sup>1</sup>, R. Magne<sup>1</sup>,  
J. Mailloux<sup>5</sup>, D. Mazon<sup>1</sup>, F. Mirizzi<sup>7</sup>, P. Mollard<sup>1</sup>, P. Moreau<sup>1</sup>,  
T. Oosako<sup>1</sup>, V. Petrzilka<sup>10</sup>, Y. Peysson<sup>1</sup>, S. Poli<sup>1</sup>, M. Prou<sup>1</sup>,  
F. Saint-Laurent<sup>1</sup>, F. Samaille<sup>1</sup>, B. Saoutic<sup>1</sup>

1) CEA, IRFM, 13108 Saint Paul-lez-Durance, France.

2) Permanent address: Institute for Plasma Research, Bhat, Gandhinagar, Gujarat, India.

3) National Fusion Research Institute, Daejeon, South Korea.

4) Southwestern Institute of Physics, Chengdu, P R China.

5) Euratom/CCFE Fusion Association, Culham Science Centre, Abingdon, OX14 3DB, UK.

6) Associação Euratom-IST, Centro de Fusão Nuclear 1049-001 Lisboa, Portugal.

7) Associazione Euratom-ENEA sulla Fusione, CR Frascati, Roma, Italy.

8) Present address: ITER Organization, 13067 Saint Paul-lez-Durance, France.

9) Institute of Plasma Physics, Chinese Academy of Sciences, Hefei, P R China.

10) Association Euratom-IPP.CR, Za Slovankou 3, 182 21 Praha 8, Czech Republic.

**Abstract.** The aim of the Tore Supra tokamak is to address physics and technology issues of long pulse discharges. For this purpose, Tore Supra is equipped with two actively cooled Lower Hybrid Current Drive (LHCD) antennas ( $f = 3.7\text{GHz}$ ), designed to operate in 1000s long pulses. One of these is the recently installed passive active multijunction (PAM) antenna, whose design is chosen for an LHCD system for ITER. The first experiments with the PAM antenna in Tore Supra have shown extremely encouraging results in terms of reflection coefficient behaviour and power handling. The maximum power and energy reached on the PAM, after  $\sim 500$  pulses on plasma, was 2.7MW during 78s (exceeding 200MJ injected energy). In addition, 2.7MW has been coupled at a plasma-antenna distance of 10cm. The coupling behaviour on the PAM, characterised by the fraction of reflected power (RC), shows good agreement with the predictions from the ALOHA coupling code. Full non-inductive discharges lasting 50s have been sustained with the PAM alone, exhibiting a current drive efficiency comparable to that of the full active multijunction antennas in Tore Supra, in similar experimental conditions.

**Keywords:** LHCD, lower hybrid, current drive, wave coupling, multijunction.

**PACS:** 52.35.Hr, 52.50.Sw, 52.55.Fa.

## INTRODUCTION AND DESCRIPTION OF THE PAM

The aim of the Tore Supra tokamak is to address physics and technology issues of long pulse discharges [1]. For this purpose, Tore Supra is equipped with two actively cooled Lower Hybrid Current Drive (LHCD) antennas ( $f = 3.7\text{GHz}$ ), designed to operate in 1000s long pulses. One of these is the recently installed passive active multijunction (PAM) antenna [2], whose design is chosen for an LHCD system for ITER [3, 4]. This design fulfils the requirements needed to withstand the heat load environment in ITER during long pulses. The PAM concept, originally proposed in [5], and further detailed in the conceptual design of an LHCD system for ITER, also exhibits low reflected power level close to the cut-off density ( $n_{co} = 3.1 \times 10^{17}\text{m}^{-3}$  at  $f = 5\text{GHz}$  and  $n_{co} = 1.7 \times 10^{17}\text{m}^{-3}$  at  $f = 3.7\text{GHz}$ ). This is an attractive feature in view of ITER, where the large plasma-wall distance may bring the density in front of the antennas to low values. As described in [6], LHCD is foreseen to be used in the second phase of ITER, where it can provide efficient volt-second saving during the plasma current ramp-up phase and assist in sustaining the advanced tokamak scenario, by driving a non-inductive current in the outer region of the plasma.

The first test of a PAM module was carried out in the FTU tokamak [7, 8]. Those experiments clearly demonstrated the possibility to operate at high power density, albeit in short pulses ( $< 1\text{s}$ ). Following this, a PAM antenna designed to inject 2.7MW for 1000s, was constructed for Tore Supra [2, 9]. This power level corresponds to a power density of  $25\text{MW/m}^2$  at  $f = 3.7\text{GHz}$  and which is equivalent to the design value of  $33\text{MW/m}^2$  at  $f = 5\text{GHz}$ , foreseen for an LHCD system in ITER [3, 4].

The PAM antenna in Tore Supra (Fig. 1) consists of 16 PAM modules, mounted in two rows and eight columns. Each PAM module has three waveguide rows, each with two active and two passive waveguides, the passive waveguides having a depth of a quarter wavelength [9]. The dimensions of the active waveguides are  $14.65\text{mm} \times 76\text{mm}$ , resulting in an active area of the antenna front face equal to  $0.11\text{m}^2$ . The PAM design allows mechanical strength to withstand disruptions and enables to put cooling channels close to the antenna front face. The Tore Supra PAM antenna is actively cooled in order to be able to operate in pulse lengths of up to 1000s, once the upgraded generator capability becomes available [10, 11, 12]. For the experiments presented here, the antenna was fed by eight old generation klystrons, each with a power capability of  $\sim 400\text{kW}$ , resulting in a total power capability of  $\sim 3\text{MW}$  injected to the plasma. From each klystron, the power is first split into two waveguides by the means of a hybrid junction, such that each klystron feeds two juxtaposed modules. Between the waveguide and the PAM module, a mode converter splits the incoming  $\text{TE}_{10}$  mode into a  $\text{TE}_{30}$  mode, with 99% conversion efficiency [9]. In view of the ITER LHCD development, a prototype of a mode converter at  $f = 5\text{GHz}$  has been constructed and tested at low power [13].

This paper presents the results obtained in the first commissioning period of the PAM antenna in Tore Supra, as well as the ongoing experiments aiming at long pulse operation at high LHCD power level (up to 4.5MW), using the two LHCD antennas.

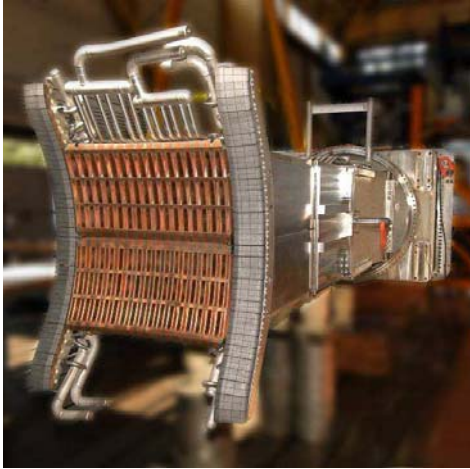


**FIGURE 1.** Front view of the Tore Supra PAM antenna before installation in the tokamak.

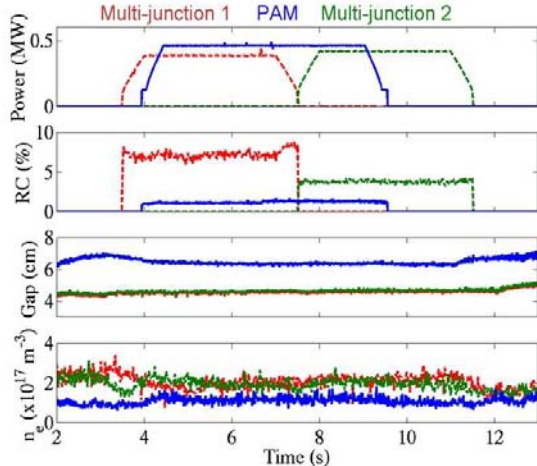


**FIGURE 2.** Comparison of the reflection coefficient (RC) on the PAM and on the full active multijunction antennas that have been used in Tore Supra.

## COUPLING EXPERIMENTS

Already on the second experimental day with the PAM antenna, the prediction of low reflected power level on the PAM was confirmed. Fig. 2 shows the comparison of the reflection coefficient obtained on the PAM antenna and on the two full active multijunction (FAM) antennas previously used in Tore Supra, in similar experimental conditions. The figure clearly shows that the PAM has lower reflection coefficient than both FAM antennas, even though the plasma-antenna distance is larger and the electron density is lower for the PAM.

Dedicated experiments and detailed analysis of the reflection coefficient (RC) behaviour of the PAM antenna has been carried out [14, 15] at low power (200kW, i.e.  $\sim 2\text{MW/m}^2$ ) in order to avoid possible non-linear effects that can occur at high power [16, 17]. In the experiments, the density at the antenna mouth was varied from  $0.5 \times 10^{17} \text{m}^{-3}$  to  $8 \times 10^{17} \text{m}^{-3}$  by varying the position of the last closed flux surface (LCFS) during the pulse. The electron density at the antenna mouth was obtained from fixed Langmuir probes, mounted on the antenna. The measured reflection coefficient, averaged over the 16 modules, exhibits a minimum around the cut-off density ( $n_{co} = 1.7 \times 10^{17} \text{m}^{-3}$  at  $f = 3.7\text{GHz}$ ) and increases as the edge density increases. This behaviour is well in agreement with the linear coupling code ALOHA [18]. This code takes into account realistic 3D antenna geometry and can cope with double electron density decay lengths ( $\lambda_n$ ) in the scrape-off layer (SOL). The first density layer ( $\lambda_{n1} \sim \text{mm}$ ) describes the private SOL between the side protections on the antenna, while the second density layer ( $\lambda_{n2} \sim \text{cm}$ ) describes the main SOL.

## HIGH POWER OPERATION

During the experimental campaigns in autumn 2009 and spring 2010, the PAM performed approximately 500 pulses on plasma. The maximum power and energy achieved on the PAM so far is 2.7MW during 78s flat-top, which results in an injected energy in a single discharge of 220MJ (Fig. 3) [19]. This record discharge was obtained after approximately 400 pulses on plasma, while the first goal of 2.7MW for shorter pulses (17s) was obtained after only 240 pulses on plasma. This power level corresponds to a power density of 25MW/m<sup>2</sup>, considering only the active surface of the antenna. It should be noted that the power limit on the PAM has not yet been fully assessed, partly due to lack of power at the generator. Once the new generation, high power CW klystrons become available on the part of the generator plant feeding the PAM, this power limit can be assessed. Up to the power level reached so far, the antenna front face protection, based on the CuXIX-line emission and infrared thermography, detected very few arcs at the antenna mouth during all the experiments with the PAM. The infrared thermography indicates that the apparent temperature of the waveguides and the side protections, which are actively cooled, remain below 270°C throughout pulse #45472.

Fig. 3 also demonstrates that high power can be coupled at large plasma-antenna distance. In #45472, the gap between the last closed flux surface (LCFS) and the antenna was increased to 10cm during the pulse. The reflection coefficient decreases slightly (from 2% to 1.5%) as the distance is increased. It has to be noted, however, that the density at the antenna is still above the cut-off density, since the plasma scenario used was characterized by long SOL density decay length ( $\lambda_n \sim 4\text{cm}$ ). This particular scenario may therefore not be considered as representative of the edge conditions that would be obtained during H-mode operation in ITER.

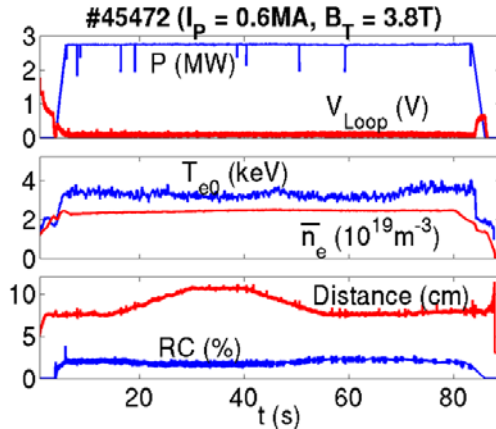


**FIGURE 3.** Maximum power and energy achieved on the PAM (2.7MW, 78s). Good coupling ( $RC < 2\%$ ) is maintained when the plasma-antenna distance is ramped to 10cm.

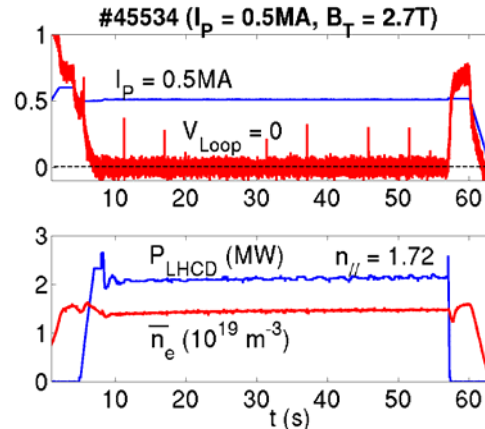


**FIGURE 4.** Full non-inductive current drive pulse, sustained with the PAM alone. The LHCD power is feedback controlled to maintain constant  $I_P$ , while  $V_{Loop}$  is kept at zero by a feedback loop on the central solenoid voltage.

## LH CURRENT DRIVE EXPERIMENTS

Full non-inductive pulses lasting up to 50s (Fig. 4) have been performed with the PAM [19], using real-time control loops to maintain the plasma current constant by adjusting the LHCD power and to maintain the primary flux consumption at zero by acting on the central solenoid voltage.  $P_{LHCD} = 2.2\text{MW}$  was required to maintain  $I_P = 0.51\text{MA}$  and  $V_{Loop} = 0$  at  $\bar{n}_e = 1.45 \times 10^{19}\text{m}^{-3}$ . The peak value of the parallel refractive index was  $n_{//} = 1.72$ , which corresponds to the optimum value, i.e. giving highest power directivity on the PAM. The value of the current drive efficiency (i.e.  $\eta_{CD} = \bar{n}_e R_0 I_{CD} / P_{CD}$ , where  $I_{CD}$  is the current driven by LHCD and  $P_{CD}$  is the coupled LHCD power) for the discharge in Fig. 4 was approximately  $0.75 \times 10^{19}\text{m}^{-2}\text{A/W}$ , taking into account a bootstrap current fraction of 10% (i.e.  $I_{CD} = 0.9 \times I_P$ ).

In these full non-inductive discharges at low density, the current drive efficiency on the PAM was found to decrease by < 10% when the density in front of the antenna was increased by a factor of two, i.e. from  $\sim 3 \times 10^{17}\text{m}^{-3}$  to  $\sim 6 \times 10^{17}\text{m}^{-3}$ . This is in agreement with the ALOHA code, that predict that the power directivity of the  $n_{//}$ -spectrum drops from 68% to 62% when the density in front of the antenna increases from  $3 \times 10^{17}\text{m}^{-3}$  to  $6 \times 10^{17}\text{m}^{-3}$ . In this edge density range, the current drive efficiency with the PAM is found to be comparable to that obtained with the FAM antennas, when using the same peak value of the  $n_{//}$ -spectrum, as for example in the GJ-discharges [20].

Experiments have also been conducted with the aim to study the current drive efficiency at high electron density (up to  $\bar{n}_e = 6 \times 10^{19}\text{m}^{-3}$ ), comparing fuelling method and effect of plasma size [21, 22, 23]. Although full non-inductive current drive could not be obtained, the evolution of the hard X-ray (HXR) emission from the non-thermal electrons produced by LHCD gives an indication of the LH current drive. For the whole range of density, a strong decay of the HXR emission is found, with density dependence very close to  $\bar{n}_e^{-2.5}$  in the 60-80keV range. At very high density ( $\bar{n}_e > 5 \times 10^{19}\text{m}^{-3}$ ), the hard X-ray emission decays even faster, in particular in the case of strong gas injection [22, 23]. This strong decay is found to be accompanied by an increase of the scrape-off-layer density fluctuations, as measured by fast acquisition of the ion saturation current on probes mounted next to the PAM antenna front [24]. Furthermore, a strong increase of the component arising from electrons with energy  $> 100\text{eV}$  was observed on the ion saturation current signal. These measurements indicate that plasma edge effects may play a role at high densities.

## MODELLING OF LH CURRENT DRIVE

The full current drive (i.e.  $V_{Loop} = 0$ ) discharge #45534, shown in Fig. 4, has been modelled with the CRONOS suite of codes [25] and the code CP3O/LUKE [26]. The CRONOS simulations uses the measured hard X-ray emission profile as input for the LH power deposition profile and reconstructs the plasma parameters, such as the flux

consumption and internal inductance. The ray-tracing code CP3O and 3D relativistic Fokker-Planck code LUKE on the other hand uses the realistic LH wave spectrum computed by the ALOHA code as input. The ray-tracing calculation uses 36 rays to describe the launched  $n_{\parallel}$ -spectrum: i.e. six  $n_{\parallel}$ -values, corresponding to the six largest peaks of the computed ALOHA  $n_{\parallel}$ -spectrum, multiplied by six poloidal launch locations, corresponding to the six waveguide rows (see Fig. 2). For this particular discharge (#45534), good agreement is obtained between the LH current profile, calculated by C3PO/LUKE and by CRONOS (based on the HXR emission profile). The two current profiles are shown in Fig. 5. In addition, quantitative agreement in the value of the LH driven current is obtained.

A further indication on the validity of C3PO/LUKE simulations for the discharge #45534 is given by the reconstruction of the line integrated hard X-ray emission signals for the horizontal chords of the fast electron bremsstrahlung diagnostic [27, 28]. Fig. 6 shows that the simulated normalized profile of the hard X-ray count rates agrees well with the experimental one, although a quantitative agreement can not be expected. However, it must be pointed out that even though C3PO/LUKE can satisfactorily reproduce the experimental results in #45534, a lack of predictability is often observed in LHCD modelling [29].

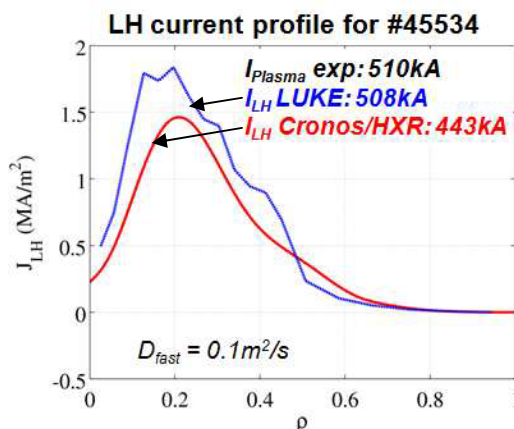


**FIGURE 5.** Simulations of the LH driven current profile for #45534, using LUKE and CRONOS/HXR.

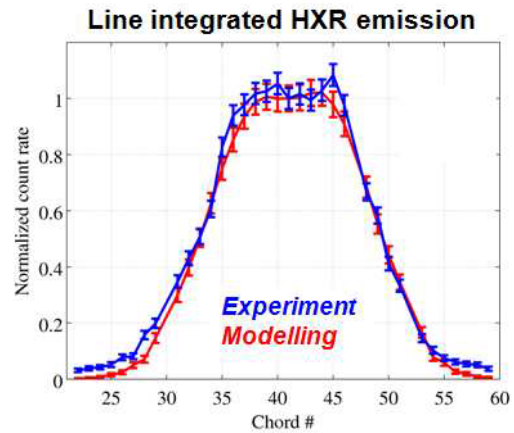


**FIGURE 6.** Experimental and simulated normalised hard X-ray count rates for #45534.

## LONG PULSE OPERATION WITH THE FULL LHCD SYSTEM

In the autumn 2010 experimental campaign, the new high power CW klystrons (TH2013C) were brought into operation on the Tore Supra plasmas [11, 12]. The klystrons, which have a specification of 700kW on matched load and 620kW on VSWR = 1.4, feed the full active multijunction antenna. So far, the klystrons have been operated up to 500kW / 10s and 440kW / 43s each, corresponding to coupled power on the FAM antenna of 3.5MW / 10s and 3.0MW / 43s, respectively. The higher available LHCD power now gives access to plasma scenarios at higher plasma

current and higher electron density. One example of the increased LH current drive capability is presented in Fig. 7, which shows a long pulse discharge at  $I_p = 0.7\text{MA}$  and  $\bar{n}_e = 2.5 \times 10^{19} \text{m}^{-3}$ , sustained for 150s with 4.5MW LHCD, using both LHCD antennas. Full non-inductive current drive has however not yet been obtained in the new parameter range. In #46569, the loop voltage was  $V_{\text{Loop}} = 40\text{mV}$  in the beginning of the pulse, and increasing to 80mV, due to an increase in electron density. The density increase is believed to be due to a non-optimised density feedback control. Further development of these scenarios is currently ongoing.

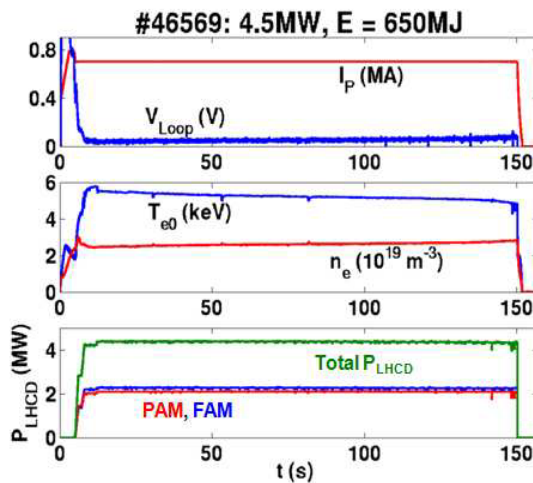


FIGURE 7. Tore Supra discharge lasting 150s, using both the PAM and FAM antennas ( $I_p = 0.7\text{MA}$ ).

## SUMMARY AND OUTLOOK

The first experiments with the ITER-relevant passive active multijunction (PAM) LHCD antenna in Tore Supra have shown extremely encouraging results in terms of reflection coefficient behaviour and power handling. Low reflected power level is obtained at low density in front of the antenna, i.e. close to the cut-off density. Very good agreement between the experimental reflection coefficient and the ALOHA code calculation is obtained. Long pulse operation at ITER-relevant power density has been demonstrated. So far,  $25\text{MW/m}^2$  (i.e.  $2.7\text{MW}$ ) has been obtained over pulse lengths up to 78s. High power ( $2.7\text{MW}$ ) has been coupled at a plasma-antenna distance of 10cm with a power reflection coefficient lower than 2%. The current drive efficiency is comparable to that of the full active multijunction (FAM) antennas, at least in conditions with low density in front of the antenna. These results give good confidence for the design of an LHCD antenna for ITER.

The upgrade of the LHCD system in Tore Supra is now near completion. The first half of the LHCD generator plant has been equipped with new high power CW klystrons, which will allow attaining 4MW coupled power on the FAM antenna. So far, 3.5MW has been obtained. Long pulse experiments at high LHCD power are

ongoing, aiming at producing fully non-inductive discharges at higher plasma current and density than obtained before [20].

## ACKNOWLEDGMENTS

The authors gratefully acknowledge the support of the Tore Supra Team, in particular of the CIMES project team. This work, supported by the European Communities under the contract of Association between EURATOM and CEA, was carried out within the framework of the European Fusion Development Agreement. The views and opinions expressed herein do not necessarily reflect those of the European Commission.

## REFERENCES

1. X. Litaudon and Tore Supra Team, *Fusion Sci. Tech.* **56** (2009) 1445.
2. D. Guilhem et al., *Fus. Eng. Des.* **86** (2011) 279.
3. Ph. Bibet et al., *Fusion Eng. Des.* **74** (2005) 419.
4. G.T. Hoang et al., *Nucl. Fusion* **49** (2009) 075001.
5. Ph. Bibet et al., *Nucl. Fusion* **35** (1995) 1213.
6. J. Decker et al., *Nucl. Fusion* **51** (2011) 073025.
7. F. Mirizzi et al., *Fusion Eng. Des.* **74** (2005) 237.
8. V. Pericoli Ridolfini et al., *Nucl. Fusion* **45** (2005) 1085.
9. J. Belo, Ph. Bibet et al., *Fusion Eng. Des.* **74** (2005) 283.
10. F. Kazarian et al., *Fusion Eng. Des.* **84** (2009) 1006.
11. L. Delpech et al., this conference.
12. G. Berger-by et al., this conference.
13. J. Hillairet et al., this conference.
14. M. Preynas et al., *Nucl. Fusion* **51** (2011) 023001.
15. M. Preynas et al., this conference.
16. O. Meneghini et al., this conference.
17. A. Ekedahl et al., in *Radio Frequency Power in Plasmas*, AIP Conf. Proc. **1187** (2009) 407.
18. J. Hillairet et al., *Nucl. Fusion* **50** (2010) 125010.
19. A. Ekedahl et al., *Nucl. Fusion* **50** (2010) 112002.
20. D. Van Houtte et al., *Nucl. Fusion* **44** (2004) L11.
21. P.K. Sharma et al., “*Hard X-ray measurements during LHCD experiments with passive active multijunction and fully active multijunction antennas in Tore Supra*”, Paper P5.184 at 37<sup>th</sup> EPS Conference on Plasma Physics, Dublin, Ireland (2010).
22. M. Goniche et al., *Plasma Phys. Control. Fusion* **52** (2010) 124031.
23. M. Goniche et al., this conference.
24. T. Oosako et al., this conference.
25. J.F. Artaud et al., *Nucl. Fusion* **50** (2010) 043001.
26. Y. Peysson and J. Decker, in *Radio Frequency Power in Plasmas*, AIP Conf. Proc. **933** (2007) 293.
27. Y. Peysson and J. Decker, *Phys. Plasmas* **15** (2008) 092509.
28. J. Decker et al., this conference.
29. Y. Peysson et al., this conference.